Adaptive Fractional Higher Interpolatory Cubature Kalman Filter with Online Noise Covariance Estimation

Jing Mu[1,*], Zihan Wu[1], Jianlian Cheng[2] and Yuanli Cai[3]

[1]*School of Compute Science and Engineering, Xi'an Technological University, Xi'an 710021, China*

[2]*School of Construction Machinery, Chang'an University, Xi'an 710064, China*

[3]*School of Electrical Engineering, Xi'an Jiaotong University, Xi'an 710049, China*

Abstract: Aiming at the challenge of state estimation in the fractional nonlinear discrete stochastic systems, we propose an adaptive fractional higher interpolatory cubature Kalman filter (AFHICKF). We develop the AFHICKF algorithm by using higher-degree interpolatory cubature rules to fulfill the numerical integral computation under the framework of Bayesian fractional filtering. Moreover, the adaptive process of AFHICKF is designed to address the state estimation problem to fractional nonlinear discrete stochastic systems with unknown noise covariance through online covariance estimation. Simulation results on reentry target tracking system verify the effectiveness, adaptiveness and superiority of the proposed filter.

Keywords: Fractional calculus, fractional nonlinear stochastic systems, higher interpolatory cubature rule, Adaptive process.

1. INTRODUCTION

Nonlinear filtering has been intensively researched in various applications such as tracking systems, navigation and signal processing [1-4]. Due to drawback of extended Kalman filter(EKF) [5], some free-derivative Kalman filters have been developed, such as unscented Kalman filter (UKF) [6], cubature Kalman Filter (CKF) [7], interpolatory cubature Kalman filters (ICKF) [8]. ICKF algorithms is developed based on the third-degree interpolatory cubature rule (ICR). In order to improve the estimation accuracy, higher-order ICKF based on fifth-degree interpolatory cubature rule is put forward.

In practice, the prior knowledge of process and measurement noise covariance is usually unknown, resulting in model mismatching. Adaptive estimation approaches are an effective way to solve the model mismatching problem. Mehra classified the adaptive estimation approaches into four categories: Bayesian, correlation, and maximum likelihood approaches and covariance matching, which is prevalent in the literature [9], such as adaptive Kalman filtering for dynamic system with outliers [1, 3, 10, 11], variational Bayesian based Kalman filtering [12], adaptive adjustment of noise covariance based Kalman filter [13], sample-based adaptive Kalman filtering [14], improved CKF [4], adaptive square-root sigma-point Kalman [15] and adaptive embedded CKF [16]. There are three types of covariance matching [17]: Q-adaptive filters for covariance of process noise [11, 18], R-adaptive filter for covariance of measurement noise [10, 17-19] and QR-adaptive filters for covariances of process and measurement noise [20-22]. Although these adaptive filters can well address the model mismatching, they still have some limitations, such as heavy computation burden and non-positive matrices, and they do not estimate covariances of both process and measurement noises online, which prevents them from being utilized in reality. Akhlaghi *et al*. proposed adaptive adjustment of noise covariance in Kalman filter for dynamic state estimation, which estimated the noise covariance online [13], and Kontoroupi *et al.* put forward another method for online estimation noise covariance using identification for joint state and noise parameter estimation of nonlinear systems [23]. The above filters obtain some promising conclusions and have advantages such as improving performance and maintaining the robustness. However, these adaptive filters were developed based on EKF and UKF.

The filters mentioned above are developed to estimate the states for integer-order nonlinear system. Recently, the fractional filters has captured a considerable attention and has been widely applied in various fields [24], such as trajectory estimation [25]. Specially, fractional EKF (FEKF) [26] play an important role in the state estimation. Then robust FEKFs are proposed for fractional discrete nonlinear system over lossy networks [27], with uncertain observations [28] and for Lévy noises [29]. Moreover, the reduced order Kalman filter [30] and fractional-order Kalman filters for

*Address correspondence to this author at the School of Compute Science and Engineering, Xi'an Technological University, Xi'an 710021, China;
E-mail: mujing@xatu.edu.cn

E-ISSN: 3083-3450/2025

colored process and measurement noises were also investigated for continuous fractional nonlinear system [31], and hybrid extended-unscented Kalman filters [32] have also been introduced. However, computation of Jacobian matrix is needed in the FEKF. Some fractional free-derivative Kalman filters such as fractional UKF(FUKF) [28], modified FUKF [33], Adaptive FUKF [34], fractional cubature Kalman filter (FCKF) [25, 35], fractional central difference Kalman filter [36], and fractional interpolatory CKFs (FICKFs) [37] have been proposed to expand fractional filters to be more general and practical. Next, some adaptive and robust fractional filters are developed for fractional nonlinear system under uncertain noise statistics, such as adaptive FUKF [38] for continuous-time nonlinear fractional-order systems [39], the modified fractional central difference Kalman filters designed for fractional nonlinear stochastic system under colored noises [40], robust fractional nonlinear state estimation against random incomplete measurements and unknown noise statistics [41], fractional higher interpolatory cubature Kalman filter (FHICKF) [42], the fractional nonlinear state estimation algorithm in non-Gaussian noise environment [43], *et al*.

Inspired by the advantages of the above-mentioned adaptive approaches and fractional filters, we develop a novel AFHICKF to estimate state including the online estimation of process and measurement noise covariances. The AFHICKF algorithm use the higher-degree interpolatory cubature rules to improve the state estimation accuracy, and address unknown noise covariance through online covariance estimation. To the best of our knowledge, AFHICKF is the first kind of filter to embrace system modeling with fractional order calculus and online noise covariance estimation. This paper has the two contributions.

- Aiming at most state estimation problems with unknown noise covariance, we propose AFHICKF algorithm including the online noise covariance estimation process and calculate its complexity;
- The simulations of reentry ballistic target (RBT) tracking in the three-dimensional coordinate system (3-D CS) have verified the effectiveness of the proposed filters. Meanwhile, the impact of various noise covariance on the performance of AFHICKF is analyzed.

The rest is organized as follows. We present fractional nonlinear discrete-time stochastic systems in Section 2. Then we describe fractional higher interpolatory cubature filter (FHICKF) with Gaussian noise and the AFHICKF with online noise covariance estimation in Section 3 and 4, respectively. In Section 5, several simulations on the state estimation of the RBT in the 3-D CS are given to verify the effectiveness, adaptiveness and superiority of the proposed filters. Furthermore, the influence of various noise covariance on the performance of AFHICKF is analyzed. Finally, the conclusion is summarized, and future work is prospected in Section 6.

2. FRACTIONAL NONLINEAR DISCRETE-TIME STOCHASTIC SYSTEMS

The definition of Grünwald–Letnikov(G-L) fractional difference is described as:

$$\Delta^{\alpha} x_k = \frac{1}{h^{\alpha}} \sum_{j=0}^{k} (-1)^j \binom{\alpha}{j} x_{k-j} \tag{1}$$

where Δ is the operator of the fractional order system, $\alpha \in \mathbb{R}$ is the fractional difference order, $\mathbb{R}$ is the set of real numbers, h is the sampling interval, and k is the sampling number for which the derivative is calculated. The coefficient $\binom{\alpha}{j}$ can be calculated as:

$$\binom{\alpha}{j} = \begin{cases} 1 & if\ j = 0 \\ \dfrac{\alpha(\alpha-1)\cdots(\alpha-j+1)}{j!} & if\ j > 0 \end{cases} \tag{2}$$

From Eq. (2), we can obtain the discrete equivalent of derivative (when $\alpha > 0$), integration (when $\alpha < 0$), and the original function (when $\alpha = 0$).

Based on the definition of G-L fractional difference, the general fractional nonlinear discrete-time stochastic systems with Gaussian noise can be described as follows:

$$\Delta^{\Upsilon} \eta_k = f(\eta_{k-1}) + w_{k-1} \tag{3}$$

$$\eta_k = \Delta^{\Upsilon} \eta_k - \sum_{j=1}^{k} (-1)^j \Upsilon_j \eta_{k-j} \tag{4}$$

$$\vartheta_k = h(\eta_k) + v_k \tag{5}$$

$$\Upsilon_j = \mathrm{diag}\left[\binom{\alpha_1}{j} \cdots \binom{\alpha_n}{j} \right] \tag{6}$$

where $\eta_k \in \mathbb{R}^{n_\eta}$ is the state vector, $f(\cdot)$ and $h(\cdot)$ are the nonlinear state equation and nonlinear measurement equation, respectively. $\vartheta_k \in \mathbb{R}^{m_y}$ is measurement. $\alpha_1, \alpha_2, \cdots, \alpha_{n_\eta}$ ($i \in \{1,2,\cdots,n_\eta\}$) are fractional system orders. w_{k-1} and v_k are process noise and measurement noise, which are uncorrelated Gaussian noises with zero means and the corresponding covariances are Q_{k-1} and N_k. We denote $\mathbb{Z}_{1:k}$ as the set of measurements up to time instant k.

To simplify the analysis, we use the following two assumptions [26], which have been widely used in the literature, such as [25, 36, 37].

Assumption 1: $E[\eta_{k-j} | \mathbb{Z}_{1:k}] \cong E[\eta_{k-j} | \mathbb{Z}_{1:k-j}]$

This assumption implies that the state estimation at instant time $k-j$ can be evaluated by using measurements $\mathbb{Z}_{1:k-j}$, and will not be updated using the newer measurements $\mathbb{Z}_{k-j:k}$.

Assumption 2: $E\left[(\hat{\eta}_{l_1} - \eta_{l_2})((\hat{\eta}_{l_1} - \eta_{l_2}))^T\right] = 0, l_1 \neq l_2$

The simplifying assumption implies the expected values of the terms $(\hat{\eta}_{l_1} - \eta_{l_1})((\hat{\eta}_{l_2} - \eta_{l_2}))^T$ ($l_1 \neq l_2$) are zero when $E[\eta_l \eta_t^T] = 0$.

3. FRACTIONAL HIGHER INTERPOLATORY CUBATURE FILTER

Bayesian fractional filters can be represented as the weighted Gaussian integral [8]. The product of a nonlinear function $g(\eta)$ and a Gaussian probability density function (PDF) $\mathcal{N}(\eta; 0, I)$ with zero mean and identity covariance is described as:

$$Integral[g] = \int g(x)\mathcal{N}(\eta; 0, I)\, d\eta \tag{7}$$

where $Integral[g]$ is an integration and $g(\eta)$ is an arbitrary non-linear function of n dimensional column vector. A $2m+1$ th-degree fully symmetric ICR $\Omega^{(m,n)}(g)$ for a n-dimensional Gaussian weighted integral can be used to approximate $Integral[g]$ as follows [44]:

$$Integral[g] \approx \Omega^{(m,n)}[g] = \sum_{p \in P^{(m,n)}} W_p^{(m,n)} g[\lambda] \tag{8}$$

Here, $P^{(m,n)}$ denotes a set of all distinct n-partitions of the integers $\{0,1,\cdots,m\}$ defined as

$$P^{(n,m)} = \left\{ (p_1, \cdots, p_n) \middle| m \geq p_1 \geq \cdots \geq p_n \geq 0, |p| \leq m \right\} \tag{9}$$

Here, p is a set of the integers $\{0,1,\cdots,m\}$ and $|p| = \sum_{i=1}^{n} p_i$. λ is defined as a generator composed by $[\lambda_{p_1}, \lambda_{p_2}, \cdots, \lambda_{p_n}]$, $\lambda_{p_i} \geq 0$, $\lambda_0 = 0$. The fully symmetric sum $g[\lambda]$ is defined as

$$g[\lambda] = \sum_{q \in \Pi_p} \sum_{s} g[s_1 \lambda_{q_1}, s_2 \lambda_{q_2}, \cdots, s_n \lambda_{q_n}] \tag{10}$$

where Π_p denotes all distinct permutations of p and the inner sum is taken over all of the sign combinations that occur when $s_i = \pm 1$ for those values of i where $\lambda_{q_i} \neq 0$. $W_p^{(m,n)}$ denotes a set of weights of generator $[\lambda]$, and is given by

$$W_p^{(m,n)} = 2^{-K} \sum_{|k| \leq m - |p|} \prod_{i=1}^{n} \frac{a_{k_i + p_i}}{\prod_{j=0, \neq p_i}^{k_i + p_i} (\lambda_{p_i}^2 - \lambda_j^2)} \tag{11}$$

where K is the number of non-zero entries in p and $a_0 = 1$, and a_i is defined as:

$$a_i = \frac{1}{\sqrt{2\pi}} \int_{-\infty}^{+\infty} e^{-\eta^2/2} \prod_{j=0}^{i-1} (\eta^2 - \lambda_j^2) d\eta \quad (i > 0) \tag{12}$$

We can use the arbitrary degree ICR in (8) to numerically compute the Gaussian weighted integrals in Gaussian filters. In the paper, in order to further improve the accuracy of computing integral in (8), we use the higher-degree ICR (HICR) namely, fifth-degree ICR to develop the proposed fractional filters. The HICR corresponds to $m = 2$ in (8), that is, $\Omega^{(2,n)}$ is polynomial with a HICR, and we know $|p| \leq 2$, then $|p| = 0$, $|p| = 1$ or $|p| = 2$.

If $|p| = 0$, the basic higher interpolatory cubature point (HICP) is $\xi_0 = [\mathbf{0}] = [0,0,\cdots,0]^T$, and its corresponding weight ($\omega_0 = W_0^{(2,n)}$) is calculated as

$$W_0^{(2,n)} = 1 - \frac{n}{\lambda_1^2} + \frac{n(n-1)}{2\lambda_1^4} + \frac{n(3-\lambda_1^2)}{\lambda_1^2 \lambda_2^2} \tag{13}$$

If $|p| = 1a$, the basic HICPs are calculated as: $\xi_i = \{\lambda_1 e_i, -\lambda_1 e_i\} (i = 1, \cdots, n)$, e_i denotes the *i*-th column of a unit matrix. Then its corresponding weights ($\omega_i = W_1^{(2,n)}$) can be calculated as

$$W_1^{(2,n)} = \frac{1}{2}\left[\frac{1}{\lambda_1^2} + \frac{3-\lambda_1^2}{\lambda_1^2(\lambda_1^2-\lambda_2^2)} + (n-1)\left(-\frac{1}{\lambda_1^4}\right)\right] \tag{14}$$

If $|p|=2$, $p_i = p_j = 1$ ($i = j$) or $p_i = 1$ is obtained. When $p_i = p_j = 1$ ($i = j$), the basic HICPs are calculated as $\xi_i = \left\{\lambda_1 s_1, -\lambda_1 s_1, \lambda_1 s_2, -\lambda_1 s_2\right\}$, the points sets ($s_1$ and s_2) are given by (15) and (16), respectively

$$s_1 \triangleq \{e_i + e_j : i < j, i, j = 1,2,\cdots,n\} \tag{15}$$

$$s_2 = \{e_i - e_j : i < j, i, j = 1,2,\cdots,n\} \tag{16}$$

Their corresponding weights ($\omega_i = W_2^{(2,n)}$) can be calculated as

$$W_2^{(2,n)} = \frac{1}{4\lambda_1^4} \tag{17}$$

When $p_i = 2$, the basic HICPs are calculated as $\xi_i = \left\{\lambda_2 e_i, -\lambda_2 e_i\right\}(i = 1,\cdots,n)$, and their corresponding weights ($\omega_i = W_3^{(2,n)}$) is calculated as:

$$W_3^{(2,n)} = \frac{3-\lambda_1^2}{2\lambda_2^2(\lambda_2^2-\lambda_1^2)} \tag{18}$$

Here, the two parameters (λ_1, λ_2) are set as two ways, one is $\lambda_1 = 1{,}356$ and $\lambda_2 = 2{,}857$, the other is $\lambda_1 = 2{,}857$ and $\lambda_2 = 1{,}356$ the two parameters selected is reasonable because the proposed the HICR with this choice of free parameters can achieve higher filtering accuracy [8].

According to the description above and the full symmetric property formulated in Eq.(10), the HICR can be formulated as：

$$\begin{aligned} Integral(g) \approx \sum_{i=1}^{N}\omega_i g(\xi_i) &= W_0^{(2,n)} g[0] + W_1^{(2,n)}\sum_{i=1}^{n}(g(\lambda_1 e_i) + g(-\lambda_1 e_i)) \\ &+ W_2^{(2,n)}\sum_{i=1}^{n(n-1)/2}\left[g(\lambda_1 s_1^{(i)}) + g(-\lambda_1 s_1^{(i)}) + g(\lambda_1 s_2^{(i)}) + g(-\lambda_1 s_2^{(i)})\right] \\ &+ W_3^{(2,n)}\sum_{i=1}^{n}(g(\lambda_2 e_i) + g(-\lambda_2 e_i)) \end{aligned} \tag{19}$$

where $W_0^{(2,n)}$, $W_1^{(2,n)}$, $W_2^{(2,n)}$ and $W_3^{(2,n)}$ are given in Eq.(13)-(14), Eq.(17) and Eq.(18). Here, $N(N = 2n^2 + 2n + 1)$ is the total number of points and .The product of a nonlinear function $g(\eta)$ and a Gaussian probability density function (PDF) $\mathcal{N}(\eta;\hat{\eta},P)$ with mean $\hat{x}$ and covariance P [45] can be expressed as:

$$Integral_{\mathcal{N}}(g) = \int g(\eta)\mathcal{N}(\eta;\hat{\eta},P)\,dx \tag{20}$$

Using Eq.(19) and (20) can be approximated as [8]:

$$Integral[g] \approx \sum_{i=1}^{N}\omega_i g(S\xi_i + \hat{\eta}) \tag{21}$$

where $P = SS^T$. S is a square root of the covariance P and it can be obtained by the Cholesky decomposition.

Above all, we can apply the HICR to approximately calculate the integrals. Then the FHICKF can be established for the fractional-order discrete nonlinear systems described in Eq.(3)-(5). The FHICKF algorithm is described as follows.

Algorithm 1: FHICKF algorithm

Sept 1. The initial state (η_0) and covariance (P_0). Repeat Step 2-3 for $k = 1,2,\cdots,M_t$ (M_t is the number of measurements).

Step 2. Assuming $\hat{\eta}_{k-1}$ and P_{k-1} are predicted state and covariance at *k*-1 time instant, respectively, and $P_{k-1} = S_{k-1}S_{k-1}^T$.

2.1. Evaluate HICPs ($i = 1,2,\cdots,N$) and propagate them through

$$X_{i,k-1} = S_{k-1}\xi_i + \hat{\eta}_{k-1} \tag{22}$$

$$X_{i,k}^* = f(X_{i,k-1}) \tag{23}$$

2.2. The predicted state $\overline{\eta}_k$

Firstly, we evaluate $\Delta^{\Upsilon}\overline{\eta}_k$ using the Eq.(21).

$$\Delta^{\Upsilon}\overline{\eta}_k \approx \sum_{i=1}^{N}\omega_i X_{i,k}^* \tag{24}$$

Then the state prediction $\overline{\eta}_k$ of η_k is obtained by

$$\overline{\eta}_k = \Delta^{\Upsilon}\overline{\eta}_k - \sum_{i=1}^{k}(-1)^j \Upsilon_j \hat{\eta}_{k-j} \tag{25}$$

2.3. The prediction covariance $\overline{P}_k$

We evaluate $P_k^{\Delta\Delta}$, $P_k^{\eta\Delta}$ and $P_k^{\Delta\eta}$ using the Eq.(21) and obtain their approximate values:

$$P_k^{\Delta\Delta} \approx \sum_{i=1}^{N} \omega_i \left[(X_{i,k}^* - \Delta^{\Upsilon}\overline{\eta}_k)(X_{i,k}^* - \Delta^{\Upsilon}\overline{\eta}_k)^T \right] + Q_{k-1} \tag{26}$$

$$P_k^{\eta\Delta} \approx \sum_{i=1}^{N} \omega_i \left[(X_{i,k-1} - \hat{\eta}_{k-1})(X_{i,k}^* - \Delta^{\Upsilon}\overline{\eta}_k)^T \right] \tag{27}$$

$$P_k^{\Delta\eta} \approx \sum_{i=1}^{N} \omega_i \left[(X_{i,k}^* - \Delta^{\Upsilon}\overline{\eta}_k)(X_{j,k-1} - \hat{\eta}_{k-1})^T \right] \tag{28}$$

The prediction covariance ($\overline{P}_k$) calculated as

$$\overline{P}_k = P_k^{\Delta\Delta} + \Upsilon_1 P_k^{\eta\Delta} + P_k^{\Delta\eta}\Upsilon_1 + \sum_{j=2}^{k} \Upsilon_j P_{k-j} \Upsilon_j \tag{29}$$

Step 3. Factorize the predicted covariance $\overline{P}_k = \overline{S}_k \overline{S}_k^T$

3.1 Calculate HICPs and propagate them through measurement equation

$$\Upsilon_{i,k} = \overline{S}_k \xi_i + \overline{\eta}_k \tag{30}$$

$$\Upsilon_{i,k}^* = h(\Upsilon_{i,k}) \tag{31}$$

3.2. Evaluate the predicted measurement, cross-covariance and innovation covariance as the following:

$$\overline{\vartheta}_k = \sum_{i=1}^{N} \omega_i \Upsilon_{i,k}^* \tag{32}$$

$$P_{\eta\vartheta,k} = \sum_{i=1}^{N} \omega_i X_{i,k} \Upsilon_{i,k}^{*T} - \overline{\eta}_k \overline{\vartheta}_k^T \tag{33}$$

$$P_{\vartheta\vartheta,k} = \sum_{i=1}^{N} \omega_i \Upsilon_{i,k}^* \Upsilon_{i,k}^{*T} - \overline{\vartheta}_k \overline{\vartheta}_k^T + N_k \tag{34}$$

3.3. Evaluate the Kalman gain, estate estimation and corresponding covariance using Eq. (35)-(37).

$$K_k = P_{\eta\vartheta,k} P_{\vartheta\vartheta,k}^{-1} \tag{35}$$

$$\hat{\eta}_k = \overline{\eta}_k + K_k(\vartheta_k - \overline{\vartheta}_k) \tag{36}$$

$$P_k = \overline{P}_k - K_k P_{\vartheta\vartheta,k} K_k^T \tag{37}$$

Here $\overline{\vartheta}_k$, $P_{\vartheta\vartheta,k}$, $P_{\eta\vartheta,k}$ and K_k are the predicted measurement, the covariance matrix of the innovation, cross covariance and Kalman gain, $\hat{\eta}_k$ and P_k are state estimation and corresponding covariance.

4. ADAPTIVE FRACTIONAL HIGHER INTERPOLATORY KALMAN FILTER

In practice, the covariances of the process and measurement noise are usually unknown. In this section, we propose the AFHICKF to deal with unknown covariances of process and measurement noise online using the covariance matching strategy, which tunes the covariance matrix of the innovation or residual based on their theoretical values. Furthermore, the numerical complexity of AFHICKF is analyzed.

4.1. Process of Adaptive Noise Covariances

The innovation error is the difference between the actual measurement and its predicted value, and the residual error is the difference between the actual measurement and its estimated value. The innovation error (ε_k) and residual error (d_k) can be calculated, respectively:

$$\varepsilon_k = \vartheta_k - \overline{\vartheta}_k \tag{38}$$

$$d_k = \vartheta_k - \hat{\vartheta}_k \tag{39}$$

Based on the above definitions, the process noise covariance estimation ($\hat{Q}_{k-1}$) and measurement noise covariance estimation ($\hat{N}_k$) can be estimated as the following.

4.1.1. Residual Based Adaptive Estimation of $\hat{N}_k$

Reformulate the innovation covariance in the Eq.(34):

$$P_{\vartheta\vartheta,k} = P_{s,k} + N_k \tag{40}$$

Here $P_{s,k} = \sum_{i=1}^{N} \omega_i \Upsilon_{i,k}^* \Upsilon_{i,k}^{*T} - \overline{\vartheta}_k \overline{\vartheta}_k^T$.

The innovation based approach estimates the measurement noise covariance matrix R_k using Eq.(40) 1:

$$R_k = P_{\vartheta\vartheta,k} - P_{s,k} \tag{41}$$

Note that theoretically speaking, N_k should be positive definite because it is a covariance matrix. Yet, its estimation in Eq.(41) could not guarantee that the estimated N_k be a positive definite matrix because the N_k is estimated by subtracting the two positive definite matrixes. Therefore, to ensure a positive definite matrix, the residual based adaptive approach proposed by [46] is used to estimate N_k . Meanwhile, we refine the adaptive process using HICR.

Factorize the covariance $P_k = S_k S_k^T$, compute the estimated measurement $\hat{\vartheta}_k$, the estimated interpolatory cubature points and the propagated interpolatory cubature points as:

$$\hat{\Upsilon}_{i,k} = S_k \xi_i + \hat{\eta}_k \tag{42}$$

$$\hat{\Upsilon}^*_{i,k} = h(\hat{\Upsilon}_{i,k}) \tag{43}$$

$$\hat{\vartheta}_k = \sum_{i=1}^{N} \omega_i \hat{\Upsilon}^*_{i,k} \tag{44}$$

$$\hat{P}_{s,k} = \sum_{i=1}^{N} \omega_i \hat{\Upsilon}^*_{i,k} \hat{\Upsilon}^{*T}_{i,k} - \hat{y}_k \hat{y}_k^T \tag{45}$$

The residual covariance can be evaluated as follows [17]:

$$E[d_k d_k^T] = N_k - \hat{P}_{s,k} \tag{46}$$

We obtain the following predicted $\bar{N}_k$:

$$\bar{R}_k = E[d_k d_k^T] + \hat{P}_{s,k} \tag{47}$$

To implement Eq.(47), the expectation operation on $E[d_k d_k^T]$ is approximated by averaging $E[d_k d_k^T]$ over time. Instead of the using the moving window, we introduces a forgetting factor $0 < \alpha \leq 1$ in Eq.(48) to adaptively estimate $\hat{N}_k$.

$$\hat{N}_k = \alpha \hat{N}_{k-1} + (1-\alpha)\bar{N}_k \tag{48}$$

Note that a larger *α* puts more weights on previous estimates and therefore incurs less fluctuation of $\hat{R}_k$, and longer time delays to catch up with changes.

4.1.2. Innovation Based Adaptive Estimation of Q_k

To adaptively estimate the Q_{k-1}, we can calculate the process noise based on Eq.(3):

$$w_{k-1} = \eta_k - f(\eta_{k-1}) + \sum_{j=1}^{k} (-1)^j \Upsilon_j \eta_{k-j} \tag{49}$$

Then we obtain:

$$\hat{w}_{k-1} = \hat{\eta}_k - f(\hat{\eta}_{k-1}) + \sum_{j=1}^{k} (-1)^j \Upsilon_j \hat{\eta}_{k-j} = \hat{\eta}_k - \bar{\eta}_x = K_k \varepsilon_k \tag{50}$$

Therefore,

$$\bar{Q}_{k-1} = E[\hat{w}_{k-1} \hat{w}_{k-1}^T] = E[K_k \varepsilon_k \varepsilon_k^T K_k^T] = K_k E[\varepsilon_k \varepsilon_k^T] K_k^T \tag{51}$$

To implement Eq.(51), the expectation operation on $E[\varepsilon_k \varepsilon_k^T]$ is approximated by averaging $E[\varepsilon_k \varepsilon_k^T]$ over time. Similar to the previous subsection 4.1.1, we use a forgetting factor α to average estimates of Q_k over time, and evaluated the $\hat{Q}_k$ as:

$$\hat{Q}_k = \alpha \hat{Q}_{k-1} + (1-\alpha)\bar{Q}_{k-1} \tag{52}$$

Given the initial condition ($\hat{\eta}_0$, P_0), the state estimation process can be recursively implemented. We summarize the AFHICKF in **Algorithm 1**.

Algorithm 1. AFHICKF algorithm

Given the state estimate $\hat{\eta}_0$ and its associated error covariance P_0 at time $k = 0$, compute the state estimate at every time k, starting with the approximation $\hat{\eta}_{k-1}$, P_{k-1} of mean and covariance of η_{k-1} given $\mathbb{Z}_{1:k-1}$.

Step 1: Initialize parameters: $\hat{\eta}_0$, P_0, $\hat{Q}_0$ $\hat{R}_0$

For $k = 1, 2, \cdots, M_t$

Step 2. Time update

Calculate the state prediction $\bar{\eta}_k$ and covariance $\bar{P}_k$ using Eq.(25) and Eq. (29).

Step 3. Measurement update

Step 3.1 Calculate the predicted measurement, the cross-covariance and innovation covariance using Eq.(32)-(34).

Step 3.2 Calculate the state estimate $\hat{\eta}_k$ and covariance P_k using Eq.(36)-(37).

Step 4. adaptive process for the process and measurement noise covariance.

$$d_k = \vartheta_k - \hat{\vartheta}_k$$

$$\varepsilon_k = \vartheta_k - \bar{\vartheta}_k$$

$$\hat{Q}_k = \alpha \hat{Q}_{k-1} + (1-\alpha)(K_k \varepsilon_k \varepsilon_k^T K_k^T)$$

$$\hat{R}_k = \alpha \hat{R}_{k-1} + (1-\alpha)(d_k d_k^T + \hat{P}_{s,k})$$

End For

4.2. Computational Complexity

Now we use floating-point operations (flops) to analyze the numerical complexity of AFHICKF. The basic arithmetic operations such as matrix addition, matrix subtraction, matrix multiplication, inverse of matrix, or square root can be referred to reference [36]. The specific flops of each step are shown in Table **1**.

Table 1: Computational Complexity of each Step

Step	Flops
$\bar{\eta}_k$	$2n_\eta^4+8\frac{1}{3}n_\eta^3+(7+2F(n_\eta))n_\eta^2+(2F(n_\eta)+2L+2)n_\eta+F(n_\eta)$
$\bar{P}_k$	$6n_\eta^4+6n_\eta^3+(L+4)n_\eta^2$
ϑ_k	$2n_\eta^4+6\frac{1}{3}n_\eta^3+(2m_y+2H(n_\eta,m_y)+5)n_\eta^2+(2m+2+2H(n_\eta,m_y))n_\eta+H(n_\eta,m_y)$
$P_{\eta\vartheta,k}$	$(6m_y-2)n_\eta^3+(6m_y-2)n_\eta^2+(5m_y-2)n_\eta$
$P_{\vartheta\vartheta,k}$	$(6m_y^2-2m)n_\eta^2+(6m_y^2-2m_y)n_\eta+6m_y^2-2m_y$
K_k	$(2m_y^2-m_y)n_\eta+m_y^3$
$\hat{\eta}_k$	$(2m_y+1)n_\eta$
P_k	$2m_yn_\eta^2+(2m_y^2-m_y)n_\eta$
$\hat{Q}_k$	$n_\eta^2+(4m_y^2-2m_y)n_\eta+m_y$
$\hat{R}_k$	$2n^4+6\frac{1}{3}n_\eta^3+5n_\eta^2+(6m_y^2+2H(n_\eta,m_y))n^2+(2H(n_\eta,m_y)+2+6m_y^2)n_\eta+H(n_\eta,m)+8m_y^2-m_y$

Here, L is memory length (in Eq. (4), η_k is related to all of the previous state and has the long memory property) when FHICKF is implemented. $F(n)$ and $H(n,m_y)$ are assumed to be the required flops of two nonlinear functions $f(\eta_{k\text{-}1})$ and $h(\eta_k)$, respectively. Their exact computational complexity is hard to evaluate but significant. The total complexity of AFHICKF is obtained by:

$$\begin{aligned}T_{AFHICKF}&=12n_\eta^4+(6m_y+25)n_\eta^3+(20+2F(n_\eta)+\\&L+4H(n_\eta,m_y)+12m_y^2+8m_y)n_\eta^2\\&+(2F(n_\eta)+2L+5+H(n_\eta,m_y)+3m_y+20m^2)n_\eta+\\&F(n_\eta)+2H(n_\eta,m_y)+m_y^3+14m_y^2-2m_y\end{aligned}\tag{53}$$

The numerical complexity of the AFHICKF is $\max\{O(n_\eta^4),O(m_y^2),O(n_\eta^2F(n_\eta)),O(n_\eta^2H(m_y,n_\eta))\}$.

Based on the below simulation analysis, the proposed AFHICKF exhibits a slightly increase in computational complexity relative to FIHCKF, FCKF, FICKF and FUKF, but it has the more estimation accuracy and robustness.

5. CASE STUDIES: RBT TRACKING IN THE 3-D CS

Now we apply the FHICKF and AFHICKF to the RBT tracking in the 3-D CS [47]. Firstly, we analyze the influence of fractional order on FHICKF. Then we have compared the performance of AFHICKF with that of FHICKF, moreover, we also have compared the performance of the AFHICKF with FUKF [28], FCKF [25] and FICKF [37]. Lastly, we analyze the influence of initial process and measurement noise covariance on the performance of AFHICKF. The platform used in the simulations is a desktop computer with Intel(R) Core (TM) i7-2620M CPU, 2.70 GHz, 6.0 GB RAM, Windows 10 professional (64 bit).

5.1. State Equation of RBT in the 3-D CS

In this paper, we consider the state estimation problem of RBT from a radar. The radar is located at the surface of the Earth (at the O_S point), the relative locations of the RBT (at the *P* point) and radar are depicted in Figure **1**. We show two orthogonal coordinate systems, one is the Earth-centered inertial coordinate system (ECI-CS, $Ox_Iy_Iz_I$), which is a right-handed system with the origin *O* at the Earth center, axis Ox_I pointing in the vernal equinox direction, axis Oz_I pointing in the direction of the North Pole *N*, and its fundamental plane Ox_Iy_I coincides with the Earth's equatorial plane. The other is orthogonal coordinate reference system named East-North-Up coordinates system (ENU-CS, O_sxyz), which has its origin at the location of the radar, z is directed along the local vertical and x and y lie in a local horizontal plane, with x pointing east and y pointing north.

We have derived the kinematics of RBT with unknown ballistic coefficient under the two hypotheses, which are that the Earth is spherical and non-rotating and that the forces acting on the target are gravity, and drag [47]. We model the kinematics of the RBT in the

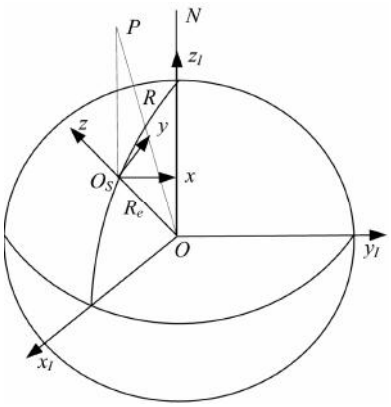

Figure 1: Geometry of radar and RBT.

ENU-CS by the following fractional discrete-time stochastic nonlinear dynamic state equation:

$$\eta_k = \Phi\eta_{k-1} + G\psi(\eta_{k-1}) - \sum_{j=1}^{k}(-1)^j \Upsilon_j \eta_{k-j} + w_{k-1} \tag{54}$$

Here, $\eta_k = [x_k\ \dot{x}_k\ y_k\ \dot{y}_k\ z_k\ \dot{z}_k\ \beta_k]^T$ is RBT's state, β_k (kg/m^2) is the ballistic coefficient, and $\Phi = Diag[\phi,\phi,\phi,1], \phi = \begin{bmatrix} 1 & T \\ 0 & 1 \end{bmatrix}$, $G = [diag[\tau,\tau,\tau],0], \tau = \begin{bmatrix} T^2/2 \\ T \end{bmatrix}$, and $\psi(x_{k-1})$ is described as:

$$\psi(x_{k-1}) = \begin{bmatrix} -\frac{\rho(h_{k-1})}{2\beta_{k-1}} V_{k-1}\,\dot{x}_{k-1} - \frac{\mu x_{k-1}}{r_{k-1}^3} \\ -\frac{\rho(h_{k-1})}{2\beta_{k-1}} V_{k-1}\,\dot{y}_{k-1} - \frac{\mu y_{k-1}}{r_{k-1}^3} \\ -\frac{\rho(h_{k-1})}{2\beta_{k-1}} V_{k-1}\,\dot{z}_{k-1} - \frac{\mu(z_{k-1}+R_e)}{r_{k-1}^3} \end{bmatrix} \tag{55}$$

here, $r_{k-1} = \sqrt{x_{k-1}^2 + y_{k-1}^2 + (z_{k-1}+R_e)^2}$, $V_{k-1} = \sqrt{\dot{x}_{k-1}^2 + \dot{y}_{k-1}^2 + \dot{z}_{k-1}^2}$ and $h_{k-1} = r_{k-1} - R_e$. T (in s) is the time interval between the radar measurements, μ ($= 3.986005\times10^{14} m^3/s^2$) and R_e ($= 6371004m$) are Earth's gravitational constant and Earth radius, respectively. $\rho(h)$ (kg/m^3) is the air density. Below 90*km* at height, it can be approximately modeled as an exponentially decaying function of height, i.e. $\rho = c_1 e^{-c_2 h}$ (c_1, c_2 are constant (dimensionless), $c_1 = 1.227$, $c_2 = 1.093\times10^{-4}$ for $h < 9144m$, and $c_1 = 1.754$, $c_2 = 1.49\times10^{-4}$ for $h \geq 9144m$) [48]. Process noise is modeled as $w_k \sim N(0, Q_k)$. We use the fractional nonlinear discrete-time stochastic systems for describing RBT's state equation in the Eq.(7) to compensate for the loss of the useful state information due to the hypothesis and obtain more accurate modeling.

The measurements including the range R_k, elevation E_k and azimuth A_k are collected by the radar. The measurement equation in the ENU-CS is described by

$$\vartheta_k = h(\eta_k) + v_k \tag{56}$$

where

$\vartheta_k = [\ R_k\ \ E_k\ \ A_k\ ]^T$,

$h(x_k) = [\ \sqrt{x_k^2 + y_k^2 + z_k^2}\ \ \arctan z_k / \sqrt{x_k^2 + y_k^2}\ \ \arctan y_k / x_k\ ]^T$

, so

$$R_k = \sqrt{x_k^2 + y_k^2 + z_k^2} + v_R \tag{57}$$

$$E_k = \arctan z_k / \sqrt{x_k^2 + y_k^2} + v_E \tag{58}$$

$$A_k = \arctan y_k / x_k + v_A \tag{59}$$

Measurement process $v_k = [\ v_R\ \ v_E\ \ v_A\ ]^T$ is modeled as the zero-mean white Gaussian noise with unknown covariance matrix N_k, σ_R, σ_E and σ_A are the error standard deviations of range, elevation and azimuth. It is independent of the process noise w_k and initial state x_0.

In the paper, we use the two-performance metrics namely, root mean-square error (RMSE) and average accumulated mean-square root error (*AMSRE*)), to evaluate the performance of the proposed filters. The definition of *RMSE* and *AMSRE* in position, velocity and ballistic coefficient at k time instant can be referred as in [47]. The results in the following simulations were obtained by RMSE and *AMSRE* averaged over 100 independent Monte Carlo runs.

5.2. Simulations and Analysis

5.2.1. Comparison of AFHICKF with FHICKF

In this subsection, we compare the performance of AFHICKF with that of FHICKF when they are applied to the state estimation of RBT tracking with unknown noise covariances. Here, the parameters $\hat{x}_0$, P_0 are the same as those in [42], the fractional order (α) is set as 10^{-6}, which has been shown that the FHICKF has better performance when the fractional order is set as $\alpha = 10^{-6}$. The initial estimated covariances are selected as

$\hat{Q}_k = 5 * Q_k$ and $\hat{R}_k = 100 * R_k$, the covariances of true process and measurement noise (Q_k and R_k) are the same as those in [42]. Figures **2-5** shows the RMSEs of FHICKF and AFHICKF in position, velocity, and the ballistic coefficient.

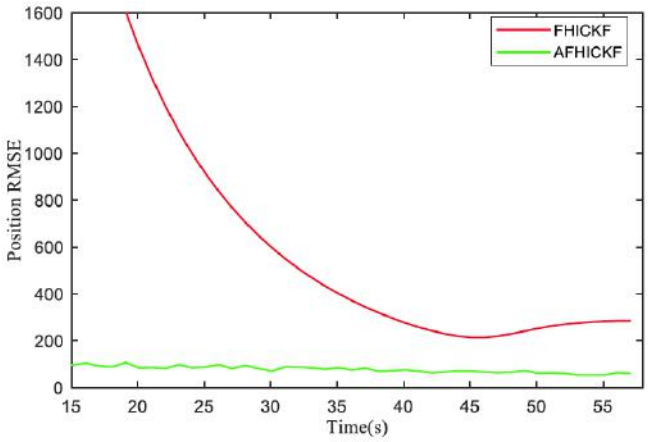

Figure 2: Position RMSE of FHICKF and AFHICKF.

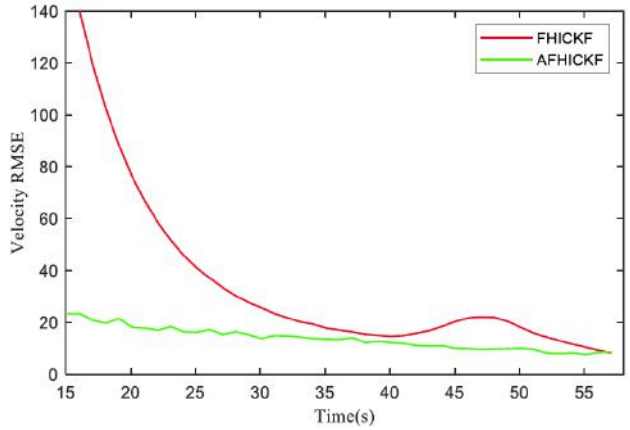

Figure 3: Velocity RMSE of FHICKF and AFHICKF.

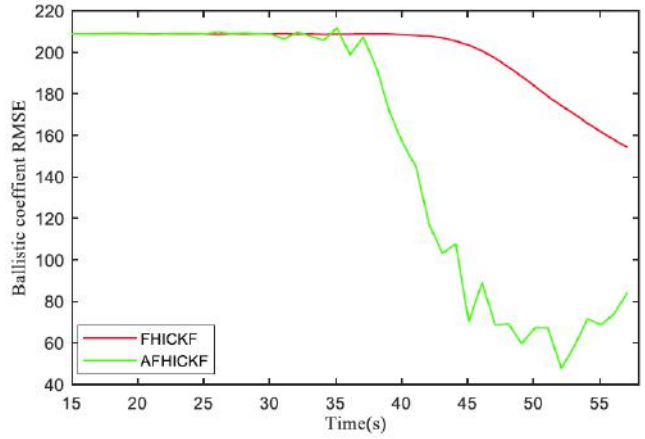

Figure 4: Ballistic coefficient RMSE of FHICKF and AFHICKF.

Obviously, in terms of effectiveness, Figures **2-4** shows the higher accuracy of AFHICKF, compared with that of FHICKF when the initial noise covariances are far from the real values.

Moreover, we compute the AMSRE*p* (AMSRE in position), AMSRE*v* (AMSRE in velocity) and AMSRE*b* (AMSRE in ballistic coefficient) for FHICKF and AFHICKF, respectively, as shown in Figure **5**. From Figure **5**, the simulation results have demonstrated the prominent improvement over AFHICKF because the AFHICKF incorporates the adaptive procedures of estimating the process and measurement noise covariance. The simulations demonstrate that the AFHICKF is an effective method to solve state estimation problem of RBT tracking with unknown noise covariances.

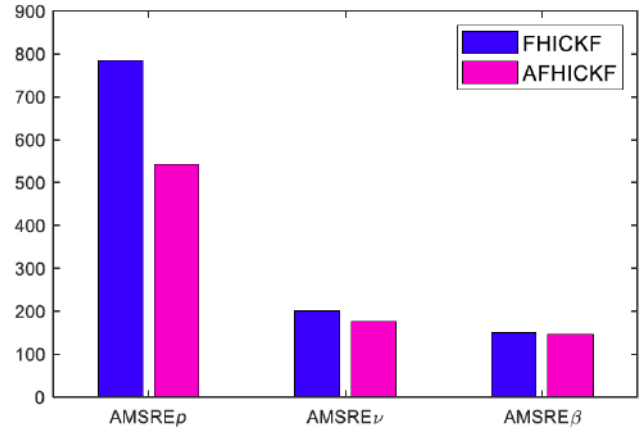

Figure 5: AMSRE of FHICKF and AFHICKF.

5.2.2. Comparison of AFHICKF with FUKF, FCKF and FICKF

In this subsection, we compare the performance of AFHICKF with that of FUKF, FCKF and FICKF when they are applied to the state estimation of RBT tracking with unknown noise covariances. Here, the parameters $\hat{x}_0$, P_0, α are the same as those in subsection 5.2.1, and the covariances (Q_k, R_k) and estimated

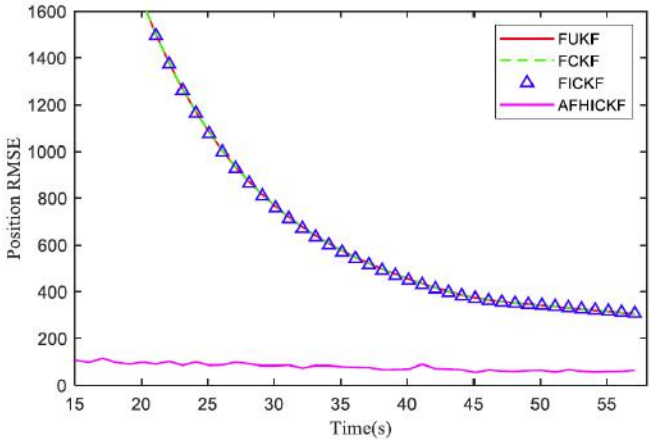

Figure 6: Position RMSE of various filters.

covariances ($\hat{Q}_k$, $\hat{R}_k$) of true process and measurement noise are the same as those in subsection 5.2.1.

From Figures **6-8**, we can see RMSEs of AFHICKF are the smallest, compared with FUKF, FCKF and FICKF. Apparently, the simulations demonstrate the effectiveness and better performance of AFHICKF. Besides, as shown in Figures **6-8**, FUKF, FCKF and FICKF have almost the same performance.

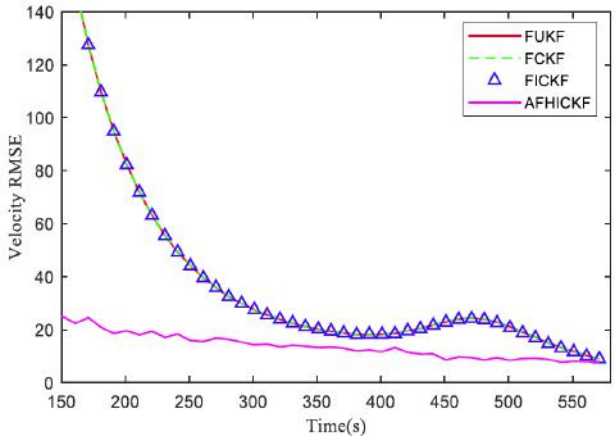

Figure 7: Velocity RMSE of various filters.

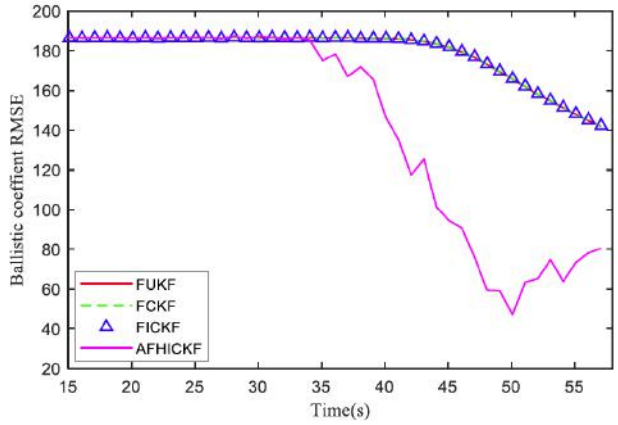

Figure 8: Ballistic coefficient RMSE of various filters.

Moreover, we compute the AMSRE*p*, AMSRE*v* and AMSRE*b* for AFHICKF and FUKF, FCKF and FICKF, respectively, as listed in Table **2**. From Table **2**, the simulation results have demonstrated the prominent improvement over AFHICKF because the AFHICKF incorporates the adaptive procedures of estimating the process and measurement noise covariance.

Table 2: AMSRE for Various Filters

Various filters	$AMSRE_p$	$AMSRE_v$	$AMSRE_b$
FUKF	1783.48	280.34	150.60
FCKF	1783.46	280.34	150.63
FICKF	1781.10	280.41	150.64
AFHICKF	257.03	159.77	144.11

5.2.4. Q and R's Adaptiveness on the Performance of AFHICKF

To evaluate the impact of Q_k and R_k on the estimation accuracy, we set Q_k and R_k by scaling Q_0 and R_0 (they are the true covariances in subsection 5.2.1). Here, the parameters $\hat{x}_0$, P_0 , α are the same as those in subsection 5.2.2. As shown in Tables **3-6**, the scaling factors are the multiples of 100. The ARMSEs of AFHICKF in position and velocity during entire tracking time are listed in Tables **3-4**, and the ARMSEs of AFHICKF in position, velocity after 5 seconds of tracking time are listed in Tables **5-6**.

Table 3: ARMSE in Position during Entire Tracking Time

AMSRE	$0.01*Q_0$	Q_0	$100*Q_0$
$0.01*R_0$	99.83	99.83	99.82
R_0	194.48	194.48	194.25
$100*R_0$	414.71	414.70	414.16

Table 4: ARMSE in Velocity during Entire Tracking Time

AMSRE	$0.01*Q_0$	Q_0	$100*Q_0$
$0.01*R_0$	104.92	104.92	104.84
R_0	143.10	143.10	142.99
$100*R_0$	188.34	188.33	188.23

Table 5: ARMSE in Position after 5 Seconds of Tracking Time

AMSRE	$0.01*Q_0$	Q_0	$100*Q_0$
$0.01*R_0$	86.56	86.56	86.57
R_0	84.03	84.03	84.04
$100*R_0$	103.27	103.27	102.90

Table 6: ARMSE in Velocity after 5 Seconds of Tracking Time

AMSRE	$0.01*Q_0$	Q_0	Q_0
$0.01*R_0$	22.16	22.16	22.18
R_0	19.78	19.78	19.77
$100*R_0$	23.88	23.88	23.78

It can be observed in Tables **3** and **5** that the ARMSE in position sharply decreases after 5 seconds of tracking time. This observation indicates that the adaptive process of covariance in the AFHICKF quickly eliminates the influence of deviation from true value

error on state estimation. From Tables **4** and **6**, we also have the same result from ARMSE in velocity. The performance improvement of the AFHICKF is more significant.

Moreover, we show the RMSEs for AFHICKF in position and velocity after 5 seconds of the tracking process in Figures **9-10**. We see RMSEs of AFHICKF in position and velocity are stable after 8 seconds of the tracking process when the initial noise and measurement covariance are various. Moreover, from simulations we also find that the RMSE of AFHICKF in ballistic coefficient has been relatively stable during the whole tracking process. Apparently, the simulations demonstrate the effectiveness and better performance of AFHICKF.

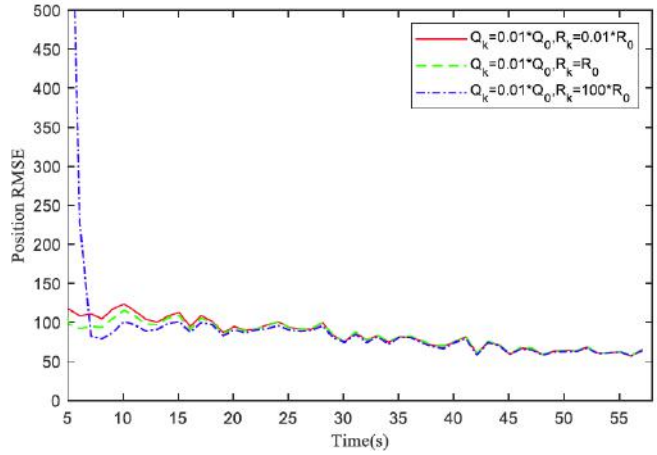

Figure 9: Position RMSE of AFHICKF with various *Q* and *R*.

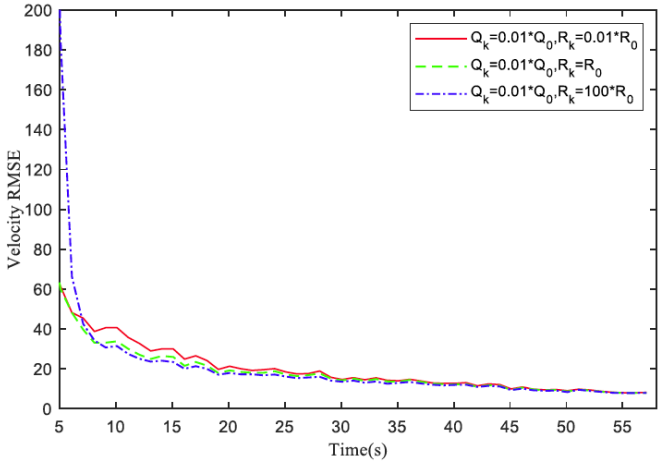

Figure 10: Velocity RMSE of AFHICKF with various *Q* and *R*.

6. CONCLUSION

The paper addresses the issue of state estimation for fractional nonlinear discrete stochastic systems with unknown noise covariances. To tackle this challenge, we propose the AFHICKF algorithms which includes process of online noise covariance estimation to estimate state. We apply AFHICKF to reentry ballistic target tracking problems with unknown noise covariance. The simulations demonstrate the AFHICKF has an improved performance, compared with the state-of-the-art fractional filters. Moreover, simulations have also shown robustness and adaptiveness when the various noise covariance is set to be larger or smaller than the true value. However, the implementation of AFHICKF algorithm involves matrix computations, which may carry the risk of matrix singularity. Moving forward, we will use square-root method to study the stability of AFHICKF algorithms and state estimation problems for fractional-order discrete-time non-linear systems with missing measurement phenomenon.

ACKNOWLEDGMENTS

This work is supported by National Natural Science Foundation of China under grant number (No.62177037).

AUTHOR CONTRIBUTIONS

Jing Mu, Zihan Wu, Jianlian Cheng and Yuanli Cai performed conceptualization, methodology, simulation analysis, validation, writing original draft and editing.

AVAILABILITY OF DATA AND MATERIAL

The data that support the findings of this study are available from the corresponding author (Mu Jing) upon reasonable request.

COMPLIANCE WITH ETHICAL STANDARDS

Conflicts of interest the authors declare that they have no conflict of interests.

REFERENCES

[1] Mohamed AH and Schwarz KP. Adaptive Kalman Filtering for INS/GPS. Joural of Geodesy, 1999, p. 193. https://doi.org/10.1007/s001900050236

[2] Ali Mehrjouyan AA. Robust adaptive unscented Kalman filter for bearings-only tracking in three dimensional case. Applied Ocean Research 2019; 87 223–232. https://doi.org/10.1016/j.apor.2019.01.034

[3] Zhu H, Zhang GR, Li YF, *et al.* An Adaptive Kalman Filter With Inaccurate Noise Covariances in the Presence of Outliers. IEEE Trans Automat Contr 2022; 67: 374-381. https://doi.org/10.1109/TAC.2021.3056343

[4] Qiu ZB and Guo L. Improved Cubature Kalman Filter for Spacecraft Attitude Estimation. IEEE Transactions on Instrumentation and Measurement 2021; 70. https://doi.org/10.1109/TIM.2020.3041077

[5] Julier S UJ, Durrant-Whyte HF. A new method for the nonlinear transformation of means and covariances in filters and estimators. IEEE Transactions on Automatic Control 2000; 45: 477-482. https://doi.org/10.1109/9.847726

[6] Simon J. Juler JKU. Unscented filtering and nonlinear estimation. Proceedings of the IEEE,2004. 92(3), p 401-422. https://doi.org/10.1109/JPROC.2003.823141

[7] Ienkaran Arasaratnam SH. Cubature Kalman Filters. IEEE Transactions on Automatic Control United States 2009, p. 1254-1269. https://doi.org/10.1109/TAC.2009.2019800

[8] Yonggang Zhang YH, Ning Li, Lin Zhao. Interpolatory cubature Kalman filters. IET Control Theory & Applications 2015; 9: 1731–1739. https://doi.org/10.1049/iet-cta.2014.0873

[9] Raman K M. Approaches to Adaptive Filtering. IEEE Transactions on Automatic Control 1972; 17: 693-698. https://doi.org/10.1109/TAC.1972.1100100

[10] Akbar Assa KNP. Adaptive Kalman Filtering by Covariance Sampling. IEEE Signal Processing Letters 2017, 24(9), p1288-1292. https://doi.org/10.1109/LSP.2017.2724848

[11] Hairong Wang ZD, Bo Feng, Hongbin Ma, Yuanqing Xia. An adaptive Kalman filter estimating process noise covariance. Neurocomputing 2017; 223: 12-17. https://doi.org/10.1016/j.neucom.2016.10.026

[12] Chang GB, Chen C, Zhang QZ, *et al*. Variational Bayesian adaptation of process noise covariance matrix in Kalman filtering. Journal of the Franklin Institute-Engineering and Applied Mathematics 2021; 358: 3980-3993. https://doi.org/10.1016/j.jfranklin.2021.02.037

[13] Akhlaghi S, Zhou N and Huang Z. Adaptive adjustment of noise covariance in Kalman filter for dynamic state estimation. In: 2017 IEEE Power & Energy Society General Meeting 16-20 July 2017 2017, pp.1-5. https://doi.org/10.1109/PESGM.2017.8273755

[14] Assa A, Janabi-Sharifi F and Plataniotis KN. Sample-based adaptive Kalman filtering for accurate camera pose tracking. Neurocomputing 2019; 333: 307-318. https://doi.org/10.1016/j.neucom.2018.11.083

[15] De Vivo F, Brandl A, Battipede M, *et al*. Joseph covariance formula adaptation to Square-Root Sigma-Point Kalman filters. Nonlinear Dynamics 2017; 88: 1987-1987. https://doi.org/10.1007/s11071-017-3406-4

[16] Zhang Y, Huang Y, Li N, *et al*. Embedded cubature Kalman filter with adaptive setting of free parameter. Signal Processing 2015; 114: 112-116. https://doi.org/10.1016/j.sigpro.2015.02.022

[17] Aritro Dey MD, Smita Sadhu, Tapan Kumar Ghoshal. Adaptive divided difference filter for parameter and state estimation of non-linear systems. IET Signal Processing, 2015, p. 369-376. https://doi.org/10.1049/iet-spr.2013.0395

[18] Jang HN, Cai YL. Adaptive Fifth-Degree Cubature Information Filter for Multi-Sensor Bearings-Only Tracking. sensors 2018. https://doi.org/10.3390/s18103241

[19] Manasi Das AD, Smita Sadhu, Tapan Kumar Ghoshal. Adaptive central difference filter for non-linear state estimation. IET Science, Measurement & Technology 2015; 9: 728-733. https://doi.org/10.1049/iet-smt.2014.0299

[20] Shan C, Zhou W, Yang Y, *et al*. Multi-Fading Factor and Updated Monitoring Strategy Adaptive Kalman Filter-Based Variational Bayesian. Sensors 2021; 21. https://doi.org/10.3390/s21010198

[21] Ali Almagbile JW, Ding WD. Evaluating the performances of adaptive Kalman filter methods in GPS/INS integration. 2010. https://doi.org/10.5081/jgps.9.1.33

[22] Li WL etl. Robust unscented Kalman filter with adaptation of process and measurement noise covariances. Digital Signal Processing 2016; 48: 93-103. https://doi.org/10.1016/j.dsp.2015.09.004

[23] Kontoroupi T and Smyth AW. Online Noise Identification for Joint State and Parameter Estimation of Nonlinear Systems. ASCE-ASME Journal of Risk and Uncertainty in Engineering Systems, Part A: Civil Engineering 2016; 2: 1-12. https://doi.org/10.1061/AJRUA6.0000839

[24] Dalir M. Bashour M. Applications of fractional calculus. Applied Mathematical Sciences 2010; 4: 1021–1032.

[25] Torabi H, Pariz N and Karimpour A. A novel cubature statistically linearized Kalman filter for fractional-order nonlinear discrete-time stochastic systems. Journal of Vibration & Control 2018; 24: 5880-5897. https://doi.org/10.1177/1077546317692943

[26] Sierociuk D eta. Fractional Kalman filter algorithm for the states, parameters and order of fractional system estimation. International Journal of Applied Mathematics and Computer Science 2006; 16: 129-140.

[27] Sun Y, Wang Y, Wu X, *et al*. Robust extended fractional Kalman filter for nonlinear fractional system with missing measurements. Journal of the Franklin Institute 2018; 355: 361-380. https://doi.org/10.1016/j.jfranklin.2017.10.030

[28] R. Caballero-Águila AH-CaJL-P. Extended and Unscented Filtering Algorithms in Nonlinear Fractional Order Systems with Uncertain Observations. Applied Mathematical Sciences 2012; 6: 1471-1486.

[29] Sun Y, Wu X, Cao J, Wei Z, Sun G. Fractional extended Kalman filtering for non-linear fractional system with Lévy noises. IET Control Theory & Applications 2017; 11: 349-358. https://doi.org/10.1049/iet-cta.2016.1041

[30] Gao Z. Reduced order Kalman filter for a continuous-time fractional-order system using fractional-order average derivative. Applied mathematics and computation 2018; 338: 72-86. https://doi.org/10.1016/j.amc.2018.06.006

[31] Gao Z. Fractional-order Kalman filters for continuous-time fractional-order systems involving colored process and measurement noises. Journal of the Franklin Institute 2018; 355: 922-948. https://doi.org/10.1016/j.jfranklin.2017.11.037

[32] Chen X, Gao Z, Ma R, Huang X. Hybrid extended-unscented Kalman filters for continuous-time nonlinear fractional-order systems involving process and measurement noises. Transactions of the Institute of Measurement and Control 2020; 42(9): 1618-1631. https://doi.org/10.1177/0142331219893788

[33] Ramezani Abdolrahman SB. A Modified Fractional-Order Unscented Kalman Filter for Nonlinear Fractional-Order Systems. Circuits, Systems, and Signal Processing 2018; 37: 3756-3784. https://doi.org/10.1007/s00034-017-0729-9

[34] Kui X, Wentao Y, Feng Q, *et al*. Adaptive fractional-order unscented Kalman filter with unknown noise statistics. International Journal of Adaptive Control and Signal Processing 2022; 36: 2519-2536. https://doi.org/10.1002/acs.3472

[35] Gao Z. Cubature Kalman filters for nonlinear continuous-time fractional-order systems with uncorrelated and correlated noises. Nonlinear Dynamics 2019; 96: 1805–1817. https://doi.org/10.1007/s11071-019-04885-y

[36] Tianyu Liu SC, Yiheng Wei, Ang Li, Yong Wang. Fractional central difference Kalman filter with unknown prior information. Signal Processing 2019; 154: 294-303. Article. https://doi.org/10.1016/j.sigpro.2018.08.006

[37] Abdolrahman Ramezani BS, Jafar Zarei. Novel Hybrid Robust Fractional interpolatory Cubature Kalman Filters. Journal of the Franklin Institute 2020; 357: 704–725. https://doi.org/10.1016/j.jfranklin.2019.11.002

[38] Xiao K, Yu W, Qu F, *et al*. Adaptive fractional-order unscented Kalman filter with unknown noise statistics. International Journal of Adaptive Control and Signal Process 2022; 36: 2519-2536. https://doi.org/10.1002/acs.3472

[39] Yang C, Gao Z, Li XN, *et al*. Adaptive fractional-order Kalman filters for continuous-time nonlinear fractional-order systems with unknown parameters and fractional-orders. International Journal of Systems Science 2021; 52: 2777-2797. https://doi.org/10.1080/00207721.2021.1904303

[40] Jiang T, Wang J, He Y, *et al*. Design of the modified fractional central difference Kalman filters under stochastic colored noises. ISA Transactions 2022; 127: 487-500. https://doi.org/10.1016/j.isatra.2021.08.044

[41] Jiang T and Wang Y. Robust Fractional Nonlinear State Estimation Against Random Incomplete Measurements and Unknown Noise Statistics. IEEE Transactions on Instrumentation and Measurement 2023; 72: 1-11. https://doi.org/10.1109/TIM.2022.3223147

[42] Mu J, Cheng JL and Xu L. Influence of Fractional order on Performance of Fractional Higher Interpolatory Cubature Kalman Filter. In: 24-th China Conference on System Simulation Technology and its Applications (CCSSTA24th), Hefei China, 2023; p. 5.

[43] Jiang T, Chen J and Wang Y. A novel fractional nonlinear state estimation algorithm in non-Gaussian noise environment. Measurement 2024; 227: 114261. https://doi.org/10.1016/j.measurement.2024.114261

[44] Genz A and Keister BD. Fully symmetric interpolatory rules for multiple integrals over infinite regions with Gaussian weight. Journal of Computational and Applied Mathematics 1996; 71: 299-309. https://doi.org/10.1016/0377-0427(95)00232-4

[45] Ienkaran Arasaratnam SH, Thomas R. Hurd. Cubature Kalman Filtering for Continuous-Discrete Systems: Theory and Simulations. IEEE Transactions on Signal Processing 2010; 58: 4977-4993. https://doi.org/10.1109/TSP.2010.2056923

[46] Wang J. Stochastic Modeling for Real-Time Kinematic GPS/GLONASS Position. Navigation 1999; 46. https://doi.org/10.1002/j.2161-4296.1999.tb02416.x

[47] Mu J and Cai Y. Likelihood-based iteration square-root cubature Kalman filter with applications to state estimation of re-entry ballistic target. Transactions Institute Measusement and Control 2012; 35: 949-958. https://doi.org/10.1177/0142331212459880

[48] Farina A, Ristic B and Benvenuti D. Tracking a ballistic target: comparison of several nonlinear filters. IEEE Transactions on Aerospace and Electronic Systems 2002; 38: 854-867. https://doi.org/10.1177/0142331212459880

Received on 19-11-2025 Accepted on 17-12-2025 Published on 31-12-2025

https://doi.org/10.65904/3083-3450.2025.01.08